Ambipolar transistors based on random networks of WS_2 nanotubes

2016 Appl. Phys. Express 9 075001

(http://iopscience.iop.org/1882-0786/9/7/075001)

OPEN ACCESS

Applied Physics Express 9, 075001 (2016)

http://doi.org/10.7567/APEX.9.075001

Ambipolar transistors based on random networks of WS_2 nanotubes

Mitsunari Sugahara[1], Hideki Kawai[1], Yohei Yomogida[1], Yutaka Maniwa[1], Susumu Okada[2], and Kazuhiro Yanagi[1]*

[1]*Department of Physics, Tokyo Metropolitan University, Hachioji, Tokyo 192-0372, Japan*
[2]*Graduate School of Pure and Applied Sciences, University of Tsukuba, Tsukuba, Ibaraki 305-8571, Japan*

*E-mail: yanagi-kazuhiro@tmu.ac.jp

Received April 21, 2016; accepted May 25, 2016; published online June 9, 2016

WS_2 nanotubes are rolled multiwalled nanotubes made of a layered material, tungsten disulfide. Their fibril structures enable the fabrication of random network films; however, these films are nonconducting, and thus have not been used for electronic applications. Here, we demonstrate that carrier injection into WS_2 networks using an electrolyte gating approach could cause these networks to act as semiconducting channels. We clarify the Raman characteristics of WS_2 nanotubes under electrolyte gating and confirm the feasibility of the injection of electrons and holes. We reveal ambipolar behaviors of the WS_2 nanotube networks in field-effect transistor setups with electrolyte gating.

Tungsten disulfide (WS_2) nanotubes are multilayered transition metal dichalcogenide nanotubes with a diameter of approximately several tens to hundreds of nanometers and a length of several micrometers [Fig. 1(a)]. WS_2 is a transition metal dichalcogenide, a layered material, and WS_2 nanotubes have a cylindrical structure formed by rolling a WS_2 sheet. Like bulk WS_2, WS_2 nanotubes are semiconducting materials with an indirect band gap similar to that of bulk WS_2 layered crystals (1–1.3 eV).[1,2] In contrast to single-walled carbon nanotubes (SWCNTs), whose properties are well known and which exhibit metallic properties with a particular chiral structure,[3] WS_2 nanotubes always exhibit semiconducting characteristics regardless of how their sheet is rolled.[4] Thus, they have great potential for use in semiconducting device applications. In addition, the rolled structure of two-dimensional sheets causes quantized conditions along the circumferential direction, inducing distinct band structures with sharp peaks in the density of states.[4–6] Theoretical calculations predict that such one-dimensional electronic structures will exhibit more distinct electrical, optical, and thermoelectric properties than two-dimensional sheets,[4–6] suggesting the uniqueness of WS_2 nanotubes. Since the discovery of WS_2 nanotubes by Tenne and coworkers in 1992,[7,8] many studies have been reported regarding their various characteristics, such as their electromechanical,[9,10] field emission,[11] field-effect,[12] optoelectronic,[13] and electrochemical properties.[14] Their fibril structures enable the fabrication of random network films, and such films are of great importance for electronic applications because of their good applicability in the fabrication of flexible and stretchable devices and printed devices, and their good scalability. However, the random networks of WS_2 nanotubes have not yet shown evidence of suitable electronic properties for applications. For example, their previously reported electronic characteristics, such as optoelectronic and field-effect properties, are limited only to a single rope of WS_2 nanotubes.[12,13] The field-effect transistor characteristics of WS_2 nanotubes in a single-rope state are indicative of an n-type transport behavior, and a relatively large mobility of $50\,cm^2\,V^{-1}\,s^{-1}$ has been revealed using back-gating approaches, indicating that electrons can be injected into WS_2 nanotubes through electric field effects.[12] However, there has not yet been any report on the field-effect properties of random networks of WS_2 nanotubes. One of the reasons for this lack is that the WS_2 nanotube networks are non-

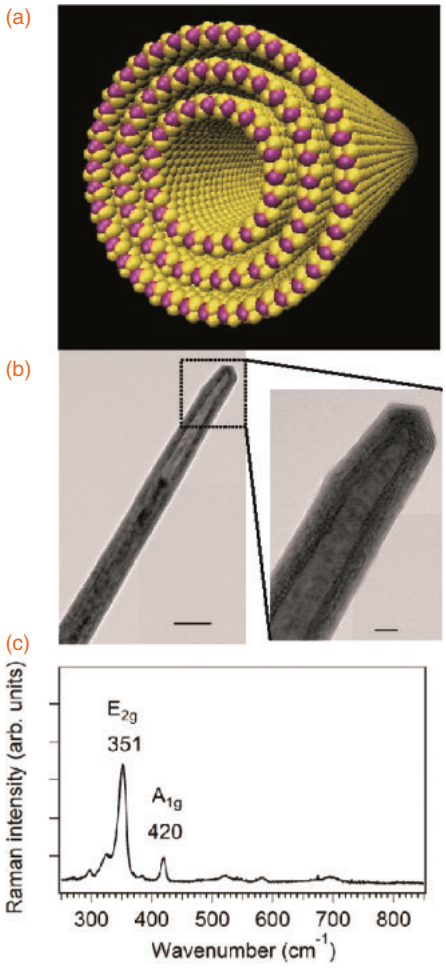

Fig. 1. (a) Schematic illustration of a multilayered WS_2 nanotube, (b) typical TEM image of one of the WS_2 nanotubes used in this study (left, the scale bar is 50 nm), and the expanded image of the end-cap region of the tube (right, the scale bar is 10 nm). For further clarification, the expanded image is shown in Fig. S1 in the online supplementary data at http://stacks.iop.org/APEX/9/075001/mmedia. (c) Raman spectrum of a sample recorded using an excitation wavelength of 561 nm.

conducting because of their relatively wide band gap, and thus cannot act as conducting channels in a random network film with a finite thickness.

Simple extensions of the back-gating approaches will be ineffective for injecting carriers into all the WS_2 nanotubes forming a random network film with a significant thickness. Previously, we manipulated various physical properties, including optical and thermoelectrical properties, of thick random network films (of approximately several hundreds of nanometers in thickness) of SWCNTs using electrolyte gating methods.[15–18] In the electrolyte gating approach, electric double layers form on the surfaces of all nanotubes constituting the network, and we can achieve carrier injection and manipulation for all nanotubes in the network. In addition, Zhang et al. previously revealed an ambipolar behavior in a single thin flake of MoS_2,[19] which is a typical transition metal dichalcogenide, using the electrolyte gating approach. An ambipolar behavior was observed in a single sheet of a thin flake of MoS_2 (15 nm thick), indicating the applicability of electrolyte gating to transition metal dichalcogenide materials. Therefore, in this study, we investigated the injection of carriers into random networks of WS_2 nanotubes using the electrolyte gating approach to reveal the electronic properties of the WS_2 random networks.

In this study, we used samples of WS_2 nanotubes purchased from Nano Materials, which were similar to those used in the field-effect study reported in Ref. 12. A typical transmission electron microscopy image of a sample nanotube is shown in Fig. 1(b) (see also Fig. S1 in the online supplementary data at http://stacks.iop.org/APEX/9/075001/mmedia). The number of walls on the left side (15 to 16) was the same as that on the right side, and the sample had an end cap structure. These features clearly indicate the tube structures of our samples. They were multilayered nanotubes with a diameter of several 10 nm and a length of approximately 1 μm. The Raman characteristics of the sample are shown in Fig. 1(c) (for an excitation wavelength of 561 nm), and as shown in the figure, we observed E_{2g} modes (351 cm^{-1}) and A_{1g} modes (420 cm^{-1}). The frequencies of these modes were consistent with those previously reported for WS_2 nanotubes.[20–22] Then, we investigated the electronic properties of WS_2 nanotube networks under carrier injection by electric double-layer formation induced by electrolyte gating using an ionic liquid.

First, we investigated the feasibility of carrier injection via electric double-layer formation using an ionic liquid for random networks of WS_2 nanotubes. Here, we investigated the Raman characteristics of random networks of WS_2 nanotubes during electrolyte gating, because if electrons or holes are properly injected into WS_2 nanotubes via electric double-layer formation, then their Raman characteristics will be significantly altered, as observed in the case of SWCNTs.[16] Figure 2(a) shows a schematic illustration of the experimental setup used for the Raman measurements. We formed gold working (W), reference (R), and gate (G) electrodes on a SiO_2 (300 nm)/Si substrate. WS_2 nanotubes were first dispersed in toluene using a bath-type ultrasonic device; the liquid solution was placed on top of the working electrode and then dried and annealed at 200 °C for 1 h in vacuum to form a WS_2 nanotube network on top of the working electrode. A scanning electron microscopy (SEM) image of a WS_2 nanotube network formed through this process is shown in Fig. 2(a). As shown in the figure, the WS_2 nanotubes formed random networks in which the WS_2 nanotubes were randomly distributed and oriented. The ionic liquid [*N*,*N*,*N*-trimethyl-*N*-propylammonium bis(trifluoromethanesulfonyl)imide, TMPA-TFSI; Kanto Kagaku] was placed in a pool surrounded by silicone rubber, and the carriers were injected into the WS_2 nanotubes by varying the potential between the working and gate electrodes using a source meter (Keithley 2636A). To evaluate the actual voltage applied to the WS_2 nanotubes, the potential difference between the reference and working electrodes, V_R, was measured simultaneously. The Raman measurements were performed using a custom-built micro-Raman measurement

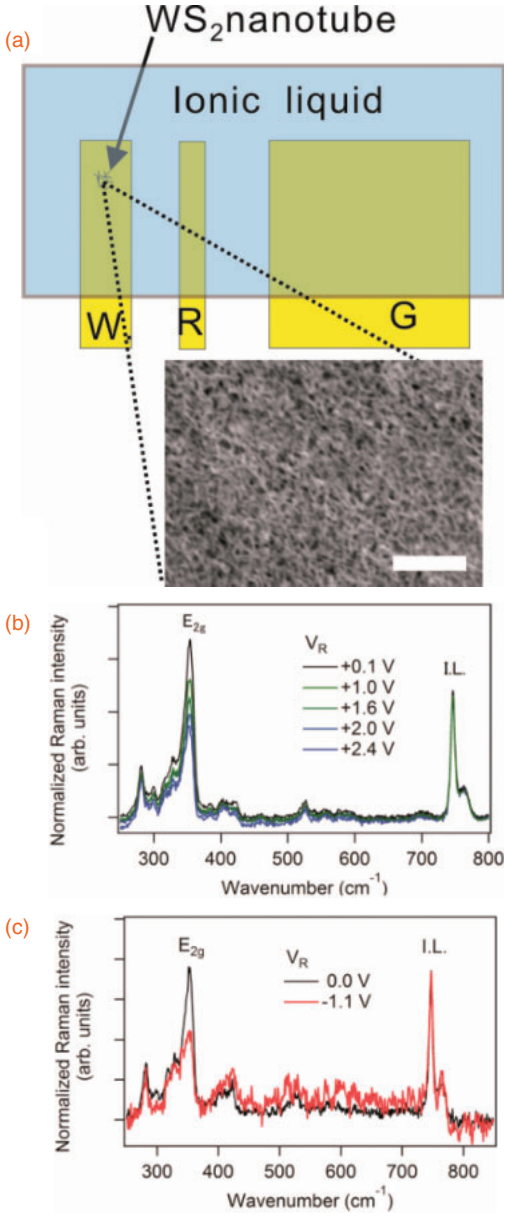

Fig. 2. (a) Schematic illustration of our setup for Raman measurements of WS_2 nanotube networks during electrolyte gating. The working (W), reference (R), and gate (G) electrodes are shown. The potential difference between the reference and working electrodes was evaluated as V_R. An SEM image of a WS_2 nanotube network formed on the top of the working electrode is shown. The scale bar represents 10 μm. (b, c) Raman spectra of the WS_2 nanotube networks at (b) positive and (c) negative V_R values. I.L. indicates the signal from the ionic liquid.

system under N_2 atmosphere at an excitation laser wavelength of 561 nm. Figures 2(b) and 2(c) show the Raman characteristics of WS_2 nanotubes at several positive and negative V_R values. Here, the Raman intensities were normalized to the peak intensity of the ionic liquid (IL) at 746 cm^{-1} to compensate for the modulation of the background signals during the measurements. In particular, in the case of hole doping, a significant increase in background signal was observed as a shift in gate voltage (see Fig. S2 in the online supplementary data at http://stacks.iop.org/APEX/9/075001/mmedia) and this background signal was removed in Fig. 2(c) to evaluate the change in the peak intensity of the E_{2g} mode of the WS_2 nanotubes with the shift in V_R. As shown here, at positive and negative V_R values, which respectively correspond to the electrons and holes injected into the WS_2 nanotubes, the E_{2g} peak intensity significantly decreased without a remarkable change in peak position. These phenomena were reversible by the shift of potential to the original position (see Fig. S2 in the online supplementary data at http://stacks.iop.org/APEX/9/075001/mmedia). Thus, we assume that the degradation by electrochemical reactions did not play a dominant role in the observed Raman spectral changes. These findings suggest that electrons and holes can be successfully injected into random networks of WS_2 nanotubes through the electric double-layer formation induced by electrolyte gating.

A decrease in the Raman intensity of the E_{2g} mode in a sheet of multi-layered transition metal dichalcogenides induced by electrochemical doping has been reported,[23] and the mechanism has been mainly attributed to the suppression of A and B optical absorption by carrier injection.[23] In this study, the excitation laser wavelength overlapped with the B exciton peak (see Fig. S3 in the online supplementary data at http://stacks.iop.org/APEX/9/075001/mmedia). Similar mechanisms might be the origin of the significant decrease in the E_{2g} mode in the Raman spectrum of WS_2 nanotubes induced by carrier injection due to electric double-layer formation. In addition, in contrast to the A_{1g} mode, it is known that the E_{2g} mode couples weakly with the electronic structure.[24,25] Thus, the peak shift of the E_{2g} mode by doping is considered to be small, and in the spectral resolution of our experimental setup, we could not identify a clear peak shift of the E_{2g} mode by carrier injection. As shown here, the results of the Raman measurements suggest that the injection of carriers through the formation of electric double-layers using an ionic liquid is applicable for random networks of WS_2 nanotubes. In addition, the results suggest the feasibility of the injection of both electrons and holes. Subsequently, we investigated the transport properties of WS_2 nanotube networks using the electrolyte gating approaches.

We fabricated WS_2 nanotube random network devices as follows. First, we fabricated source (S), drain (D), gate (G), and reference (R) electrodes on the SiO_2 (300 nm)/Si substrates. To form a film of random networks of WS_2 nanotubes to serve as a channel, the WS_2 nanotubes were first dispersed in toluene, and the dispersed solution was then sprayed onto the substrate between the source and drain electrodes. A photograph of a typical device is shown in Fig. 3(a). The channel length and width were 80 μm and 3.7 mm, respectively. The transport characteristics were measured using a prober system (Nagase Grail 10). The measurements were

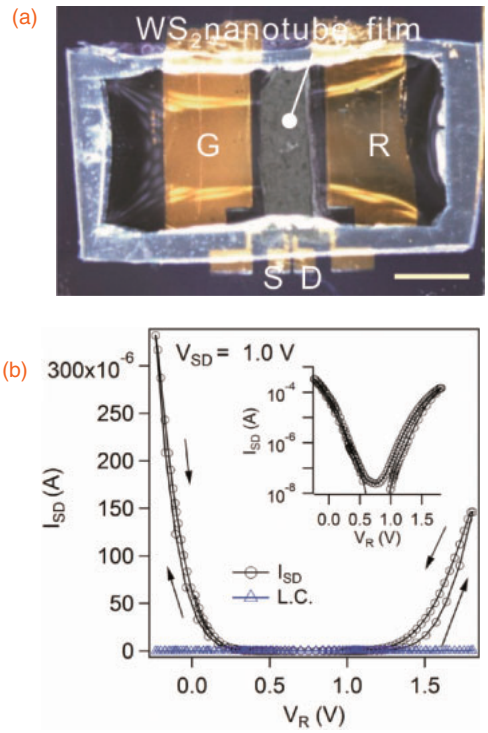

Fig. 3. Photograph of a typical transistor device structure consisting of a thick WS_2 nanotube random network film in an electrolyte gating setup. The source (S), drain (D), gate (G), and reference (R) electrodes are shown. The scale bar represents 2 mm. (b) Transport characteristics of the device. The circles represent the current I_{SD} between the source and drain electrodes. I_{SD} is plotted as a function of the potential difference between the source and reference electrodes, V_R. Blue triangles represent the amount of leakage current, LC, detected in the gate electrode. The inset presents a log plot of the transport characteristics.

performed in vacuum (10^{-3} Pa) at room temperature. Figure 3(b) shows the transport characteristics of the device. The source–drain current I_{SD} is plotted as a function of the potential difference between the reference and source electrodes, V_R, at a bias voltage V_{SD} of 1.0 V. Remarkably, we observed a clear ambipolar behavior of the random network of WS_2 nanotubes. The leakage current (LC) at the gate electrode was on the order of 10^{-8} A. The I_{SD} in the On state was on the order of 10^{-6} A, providing good evidence of the transport of holes and electrons in the channel. The observed ambipolar behavior clearly indicated the accumulation of holes and electrons on the WS_2 nanotube networks induced by electrolyte gating approaches. The inset of Fig. 3(b) shows a log plot of the transport results. The on/off ratio reached nearly 10^4. To assess the carrier mobility of this device, we used the following standard formula to evaluate the carrier mobility: $\mu = dI_{SD}/dV_R \cdot L/(CWV_{SD})$. Here, L is the channel length, W is the channel width, and C is the specific capacitance. The capacitance in this experimental setup was measured using an impedance analyzer (BAS ALS model 611ES). The highest hole mobility was estimated to be 3.6 $cm^2 V^{-1} s^{-1}$, and the electron mobility was 0.3 $cm^2 V^{-1} s^{-1}$. These values are small compared with the reported electron mobility in a single rope of WS_2 nanotubes (50 $cm^2 V^{-1} s^{-1}$)[12] and are also small compared with the reported mobility in a single thin flake of MoS_2 [44 (p-type) or 86 (n-type) $cm^2 V^{-1} s^{-1}$].[19] This low mobility can be attributed to the presence of numerous junctions between the

nanotube contacts; however, the mobility values are comparable to that for amorphous Si ($\sim 1\,cm^2\,V^{-1}\,s^{-1}$),[26] which is commonly used in thin-film transistor applications, indicating that random networks of WS_2 nanotubes show good potential for such applications.

Random networks of SWCNTs have been used in various electronic applications.[27] However, SWCNTs unfortunately exhibit metallic conduction in certain specific structures, and the presence of metallic SWCNTs causes their field-effect transistor performance to degrade. The question of how to remove metallic SWCNTs has been treated as a central concern for their use in semiconducting device applications. However, in the case of WS_2 nanotubes, although they are multilayered, they all act as semiconductors regardless of their chirality.[4] Thus, they demonstrate great advantages for use in semiconducting device applications. In addition, theoretical calculation indicates that the rolled structure of two-dimensional sheets causes quantized conditions along the circumferential direction and forms distinct band structures with sharp peaks in the density of states.[4–6] Unfortunately, the diameters of WS_2 nanotubes we used here are several 10 nm and the sample is in a mixed state of various different structures; thus, it is difficult to observe unique physical properties reflecting one-dimensional cylindrical structures. However, the observed ambipolar behavior in WS_2 nanotube random networks will pave the way toward electronic device applications using inorganic nanotubes and stimulate further investigation of inorganic nanotubes with a selected electronic structure.

Acknowledgments This work was partially supported by MEXT KAKENHI Grant Number 25246006 and JSPS KAKENHI Grant Number 16H00919.

1) J. A. Wilson and A. D. Yoffe, Adv. Phys. **18**, 193 (1969).
2) W. Zhao, Z. Ghorannevis, L. Chu, M. Toh, C. Kloc, P. Tan, and G. Eda, ACS Nano **7**, 791 (2013).
3) R. Saito, M. Fujita, G. Dresselhaus, and M. Dresselhaus, Appl. Phys. Lett. **60**, 2204 (1992).
4) G. Seifert, H. Terrones, M. Terrones, G. Jungnickel, and T. Frauenheim, Solid State Commun. **114**, 245 (2000).
5) K. Chen, X. Wang, D. Mo, and S. Lyu, J. Phys. Chem. C **119**, 26706 (2015).
6) J. Xiao, M. Long, X. Li, H. Xu, H. Huang, and Y. Gao, Sci. Rep. **4**, 4327 (2014).
7) R. Tenne, L. Margulis, M. Genut, and G. Hodes, Nature **360**, 444 (1992).
8) Y. Feldman, E. Wasserman, D. J. Srolovitz, and R. Tenne, Science **267**, 222 (1995).
9) M. Ghorbani-Asl, N. Zibouche, M. Wahiduzzaman, A. F. Oliveira, A. Kuc, and T. Heine, Sci. Rep. **3**, 2961 (2013).
10) D. Maharaj and B. Bhushan, Sci. Rep. **5**, 8539 (2015).
11) G. Viskadouros, A. Zak, M. Stylianakis, E. Kymakis, R. Tenne, and E. Stratakis, Small **10**, 2398 (2014).
12) R. Levi, O. Bitton, G. Leitus, R. Tenne, and E. Joselevich, Nano Lett. **13**, 3736 (2013).
13) C. Zhang, S. Wang, L. Yang, Y. Liu, T. Xu, Z. Ning, A. Zak, Z. Zhang, R. Tenne, and Q. Chen, Appl. Phys. Lett. **100**, 243101 (2012).
14) K. Xu, F. Wang, Z. Wang, X. Zhang, Q. Wang, Z. Cheng, M. Safdar, and J. He, ACS Nano **8**, 8468 (2014).
15) K. Yanagi, R. Moriya, Y. Yomogida, T. Takenobu, Y. Naito, T. Ishida, H. Kataura, K. Matsuda, and Y. Maniwa, Adv. Mater. **23**, 2811 (2011).
16) K. Yanagi, R. Moriya, N. T. Cuong, M. Otani, and S. Okada, Phys. Rev. Lett. **110**, 086801 (2013).
17) K. Yanagi, S. Kanda, Y. Oshima, Y. Kitamura, H. Kawai, T. Yamamoto, T. Takenobu, Y. Nakai, and Y. Maniwa, Nano Lett. **14**, 6437 (2014).
18) T. Igarashi, H. Kawai, N. Cuong, S. Okada, T. Pichler, and K. Yanagi, Phys. Rev. Lett. **114**, 176807 (2015).
19) Y. Zhang, J. Ye, Y. Matsuhashi, and Y. Iwasa, Nano Lett. **12**, 1136 (2012).
20) P. M. Rafailov, C. Thomsen, K. Gartsman, I. Kaplan-Ashiri, and R. Tenne, Phys. Rev. B **72**, 205436 (2005).
21) M. Viršek, A. Jesih, I. Milošević, M. Damnjanović, and M. Remškar, Surf. Sci. **601**, 2868 (2007).
22) G. L. Frey, R. Tenne, M. Matthews, M. Dresselhaus, and G. Dresselhaus, J. Mater. Res. **13**, 2412 (1998).
23) Y. Wang, J. Z. Ou, S. Balendhran, A. F. Chrimes, M. Mortazavi, D. D. Yao, M. R. Field, K. Latham, V. Bansal, J. R. Friend, S. Zhuiykov, N. V. Medhekar, M. S. Strano, and K. Kalantar-zadeh, ACS Nano **7**, 10083 (2013).
24) B. Chakraborty, A. Bera, D. Muthu, S. Bhowmick, U. Waghmare, and A. Sood, Phys. Rev. B **85**, 161403 (2012).
25) G. Frey, R. Tenne, M. Matthews, M. Dresselhaus, and G. Dresselhaus, Phys. Rev. B **60**, 2883 (1999).
26) B. Stannowski, R. Schropp, R. Wehrspohn, and M. Powell, J. Non-Cryst. Solids **299–302**, 1340 (2002).
27) E. Snow, J. Novak, P. Campbell, and D. Park, Appl. Phys. Lett. **82**, 2145 (2003).